



Sensitivity of urban hydrodynamic modelling

G. Bruni et al.

This discussion paper is/has been under review for the journal Hydrology and Earth System Sciences (HESS). Please refer to the corresponding final paper in HESS if available.

On the sensitivity of urban hydrodynamic modelling to rainfall spatial and temporal resolution

G. Bruni¹, R. Reinoso², N. C. van de Giesen¹, F. H. L. R. Clemens^{1,3}, and J. A. E. ten Veldhuis¹

¹Department of Water Management, Faculty of Civil Engineering and Geosciences, Delft University of Technology, the Netherlands

²Department of Geoscience and Remote Sensing, Faculty of Civil Engineering and Geosciences, Delft University of Technology, the Netherlands

³Deltares, Delft, the Netherlands

Received: 13 May 2014 – Accepted: 22 May 2014 – Published: 6 June 2014

Correspondence to: G. Bruni (g.bruni@tudelft.nl)

Published by Copernicus Publications on behalf of the European Geosciences Union.

Title Page

Abstract

Introduction

Conclusions

References

Tables

Figures



Back

Close

Full Screen / Esc

Printer-friendly Version

Interactive Discussion



Abstract

Cities are increasingly vulnerable to floods generated by intense rainfall, because of their high degree of imperviousness, implementation of infrastructures, and changes in precipitation patterns due to climate change. Accurate information of convective storm characteristics at high spatial and temporal resolution is a crucial input for urban hydrological models to be able to simulate fast runoff processes and enhance flood prediction. In this paper, a detailed study of the sensitivity of urban hydrological response to high resolution radar rainfall was conducted. Rainfall rates derived from X-band dual polarimetric weather radar for four rainstorms were used as input into a detailed hydrodynamic sewer model for an urban catchment in Rotterdam, the Netherlands. Dimensionless parameters were derived to compare results between different storm conditions and to describe the effect of rainfall spatial resolution in relation to storm and hydrodynamic model properties: rainfall sampling number (rainfall resolution vs. storm size), catchment sampling number (rainfall resolution vs. catchment size), runoff and sewer sampling number (rainfall resolution vs. runoff and sewer model resolution respectively). Results show catchment smearing effect for rainfall resolution approaching half the catchment size, i.e. for catchments sampling numbers greater than 0.5 averaged rainfall volumes decrease about 20%. Moreover, deviations in maximum water depths, from 10 to 30% depending on the storm, occur for rainfall resolution close to storm size, describing storm smearing effect due to rainfall coarsening. Model results also show the sensitivity of modelled runoff peaks and maximum water depths to the resolution of the runoff areas and sewer density respectively. Sensitivity to temporal resolution of rainfall input seems low compared to spatial resolution, for the storms analysed in this study. Findings are in agreement with previous studies on natural catchments, thus the sampling numbers seem to be promising as an approach to describe sensitivity of hydrological response to rainfall variability for intra-urban catchments and local convective storms. More storms and different urban catchments of varying characteristics need to be analysed in order to validate these findings.

Sensitivity of urban hydrodynamic modelling

G. Bruni et al.

[Title Page](#)

[Abstract](#)

[Introduction](#)

[Conclusions](#)

[References](#)

[Tables](#)

[Figures](#)



[Back](#)

[Close](#)

[Full Screen / Esc](#)

[Printer-friendly Version](#)

[Interactive Discussion](#)



1 Introduction

Rainfall is the key input to the majority of hydrological models, and a crucial issue for hydrologists is to find the importance of the spatial structure of rainfall and its representation for flood generation (Segond et al., 2007). Many studies have been conducted in large natural catchments, revealing that spatial variability of rainfall is important in determining both the timing and volume of the rainfall transformed into runoff (Obled et al., 1994) and thus the timing of the simulated basin response and the magnitude of the response peak (Dawdy and Bergman, 1969; Krajewski et al., 1991; Seliga et al., 1992). It has been suggested, with much less evidence, that this is also true for small catchments with smaller response times, such as urban catchments (Blanchet et al., 1992; Obled et al., 1994). Urban catchments are characterised by a high percentage of imperviousness, which leads to a high proportion of the rain producing runoff. It is therefore expected that the effect of spatial rainfall variability on water flows is greater in urban catchments than in rural ones. Here local variation of rainfall input is smoothed and delayed within the soil due to the infiltration occurring in pervious areas, as it was found by Obled et al. (1994), among others. A first conclusion emerging from previous studies is that urban catchments, characterized by a fast hydrological response due to both low interception and infiltration, are highly sensitive to the small-scale spatial and temporal variability of the precipitation field (Bell and Moore, 2000; Einfalt et al., 2004; Gires et al., 2013, among others). Moreover, the hydrological community has so far focused on flood modelling (Schmitt et al., 2004; Balmforth and Dibben, 2006; Parker et al., 2011; Pathirana et al., 2011; Priest et al., 2011; Neal et al., 2012; Ozdemir et al., 2013), and only recently has been focusing on the impact of rainfall variability on hydrodynamic models (Gires et al., 2012; Liguori et al., 2012; Vieux and Imgarten, 2012).

As a consequence, rainfall variability information is a critical component to study hydrological response in urban drainage systems using hydrological models. Weather radars are more suitable for this purpose than rain gauges as they have better spatial

HESSD

11, 5991–6033, 2014

Sensitivity of urban hydrodynamic modelling

G. Bruni et al.

[Title Page](#)

[Abstract](#)

[Introduction](#)

[Conclusions](#)

[References](#)

[Tables](#)

[Figures](#)



[Back](#)

[Close](#)

[Full Screen / Esc](#)

[Printer-friendly Version](#)

[Interactive Discussion](#)



coverage. Weather radars, such as S-band and C-band radars, are already used by meteorological institutes worldwide in order to (indirectly) measure and predict precipitation at national and regional scales. Nonetheless, several studies have shown that the spatial resolution of operational radar network measurements is insufficient to meet the scale of urban hydrodynamics (Berne et al., 2004; Emmanuel et al., 2011; Schellart et al., 2011). Because of their relatively low cost and small size, X-band radars are ideally suited for local rainfall estimation. These radars measure at high resolutions, both in space and time, and much closer to the ground than S- or C-band radars. X-band radars have been tested locally and show better performances in catching the rapidly changing characteristics of intense rainfall than rain gauges (Jensen and Pedersen, 2005). This is particularly the case when the distance between rain gauges is larger than 3–4 km (Wood et al., 2000). This study uses rainfall estimates from dual-polarimetric X-band radar (IDRA), operated by Delft University of Technology (TU Delft), and located at Cabauw Experimental Site for Atmospheric Research (CESAR) (Leijnse et al., 2010; Otto and Russchenberg, 2011). X-band rainfall estimates inputted into a dual drainage model will help to answer the following questions:

- Does small-scale precipitation variability affect hydrological response and can an urban drainage model properly describe such a response?
- Is high spatial resolution rainfall information required when storm does not present pronounced variability?
- Does sensitivity of small sized urban catchments to spatial and temporal variability of precipitation depend on catchment scale?

It has been found that for natural catchments, the scale of rainfall representation is directly related to the scale of the spatial variability of the storm and the size of the catchment that collects rainwater and transforms it into runoff (Krajewski et al., 1991; Ogden and Julien, 1994; Winchell et al., 1998; Koren et al., 1998, among others). The purpose of this paper is to analyse the sensitivity of a semi-distributed hydrodynamic

HESSD

11, 5991–6033, 2014

Sensitivity of urban hydrodynamic modelling

G. Bruni et al.

[Title Page](#)

[Abstract](#)

[Introduction](#)

[Conclusions](#)

[References](#)

[Tables](#)

[Figures](#)



[Back](#)

[Close](#)

[Full Screen / Esc](#)

[Printer-friendly Version](#)

[Interactive Discussion](#)



model to rainfall spatial and temporal resolutions derived from weather radar data at intra-urban scale, according to spatial characteristics of both storm and catchment, and also according to model topology. Sensitivity is quantified using dimensionless parameters that describe the relationship between rainfall resolution and spatial characteristics of the urban catchment, storm cells and model topology. The findings have relevance for the use of high resolution radar data in flood forecasting and flood protection in cities, at intra-urban scale. It provides a contribution to the debate on radar spatial resolution requirements for urban drainage modelling of small-scale urban catchments at district level, i.e. up to 3 km². The paper is organised as follows. Section 2 presents the case study, hydrodynamic modelling approach as well as the analysis and description of rainfall fields used to conduct the sensitivity analysis. In Sect. 3 scale lengths are first defined and then used to obtain a set of dimensionless parameters that will characterize the relationship between rainfall fields, spatial resolution of rainfall and catchment characteristics. In Sect. 4 results of the scale analysis are shown and discussed. Lastly, conclusions are presented in Sect. 5.

2 Presentation of the dataset

2.1 Case study and model description

This paper focusses on the Central district of Rotterdam, the Netherlands. The district is densely populated and includes mainly residential areas of approximately 30 000 people, as well as business and shopping centres. The district size ranges 3.4 km². Two green areas are located in the southern part of the district, sized 6 and 24 ha. The southern border of the district is formed by the Meuse River. The district belongs to a polder area below sea level. For this reason, during heavy rainfall, excess storm water needs to be pumped out into the river system or temporally stored elsewhere. An underground storage facility with a capacity of 10 000 m³ has been built in the district to reduce flood risk during heavy rainfall events.

HESSD

11, 5991–6033, 2014

Sensitivity of urban hydrodynamic modelling

G. Bruni et al.

Title Page

Abstract

Introduction

Conclusions

References

Tables

Figures

◀

▶

◀

▶

Back

Close

Full Screen / Esc

Printer-friendly Version

Interactive Discussion



Sensitivity of urban hydrodynamic modelling

G. Bruni et al.

Title Page

Abstract

Introduction

Conclusions

References

Tables

Figures

⏪

⏩

◀

▶

Back

Close

Full Screen / Esc

Printer-friendly Version

Interactive Discussion



A sewer model has been built for the catchment using Sobek-urban (Deltares, 2014). The combined sewer system was modelled in 1-D and consists of around 3000 manhole nodes (most of them are with runoff) and 11 external weirs, which serve as outflow points. The model contains four pressurized pipes interconnecting parts of the sewer system. Two external pumping stations transport water to the waste water treatment plant and to the river. Rainfall–runoff processes are modelled in Sobek RR (Deltares, 2014). The main components in this model are surface water storage, evaporation, infiltration and delay of surface runoff before entering the sewer system. Surface water storage occurs when rainwater form puddles. When the water level exceeds the given maximum street storage, runoff is generated. Infiltration is computed on pervious surfaces by Horton equation. Runoff to the sewer system is computed as a function of net rainfall and runoff factors, which depend on length, roughness, slope and percentage of imperviousness of the areas. According to Dutch guidelines (Stichting RIONED, 2004), four different area types were used with different sets of runoff parameter values (Table 1): closed paved, open paved, roof flat and roof sloped (with slope larger than 4 %) areas. The open paved area type represents paved streets with bricks, which allow water to infiltrate and to be retained within the road surface. Green areas are not taken into account by the model, as they are assumed to be disconnected from the sewer system. The rainfall–runoff module is lumped and its basic unit is the “runoff area”. Each runoff area contains different types of surface, the runoff of which enters the sewer system through the manhole nodes.

2.2 Rainfall data

Four rainfall storms were selected for analysis. According to the classification adopted by Emmanuel et al. (2012), they have been grouped as follows:

- Event 1 and Event 2: storm organized in rain bands
- Event 3: storm less organized

– Event 4: light rain

In Event 1, a long lived squall line was measured on 3 January 2012. A squall line is a line of convective cells that forms along a cold front with a predominately trailing stratiform precipitation (Storm et al., 2007). Squall lines are typically associated with a moderate shear between 10 and 20 m s⁻¹ and strong updraft (Weisman and Rotunno, 2004). If winds increase rapidly with height ahead of a strong front, thunderstorms triggered along the boundary may organize into severe storms called supercell storms. The X-band radar was able to capture storm features associated with supercell. Event 2 can be characterised as a cluster of convective and organized storm cells that moved in north-east direction. It was detected on 10 September 2011. The storm system showed a convective spread area larger than the first event and with slower shift. In Event 3, occurred on 28 June 2011 and mesoscale observations showed a non-organized squall line moving north east and containing rainfall rate cores of at least 10 mm h⁻¹. X-band radar rainfall estimates were based on both horizontal reflectivity and specific differential phase. Rainfall rate values of 50 mm h⁻¹ were founded over small areas of 25 km² during 22:00–23:00 UTC. Lastly, Event 4 is a stratiform precipitation moving slowly toward the east and showing uniform rainfall rates. Rainfall retrieval was based on reflectivity only, of about 8 mm h⁻¹. Main characteristics of the four events are summarized in Fig. 1a. Figure 1b shows maximum rainfall intensity for spatial aggregation levels of 100, 500 and 1000 m for Event 1. Aggregations were made from radar rainfall rates at 30 m polar pixels based on reflectivity for values smaller than 30dBZ, differential phase otherwise (Otto and Russchenberg, 2011). The spatial resolutions that were considered are: 100, 500, 1000 and 2000 m. No plots of the 2000 m-scale were shown, as it results in a uniform rainfall over the entire study area. Rainfall plots show rainfall gradient smoothing and storm core displacement along the three spatial aggregation levels.

Sensitivity of urban hydrodynamic modelling

G. Bruni et al.

[Title Page](#)

[Abstract](#)

[Introduction](#)

[Conclusions](#)

[References](#)

[Tables](#)

[Figures](#)



[Back](#)

[Close](#)

[Full Screen / Esc](#)

[Printer-friendly Version](#)

[Interactive Discussion](#)



3 Methods

The effects of radar spatial resolution on hydrological model outputs by means of length scales were first addressed by Ogden and Julien (1994). In their study, they aimed to explain variability in hydrological responses based on rainfall and catchment characteristics. To this end, they introduced various length scales to characterize rainfall data and catchments, such as de-correlation length of the storm, grid size of rainfall data, characteristic length of the catchment, and grid size of runoff model. In this framework, Ogden and Julien (1994) give recommendations for medium size natural catchments: they recommended rainfall spatial resolution of 0.4 the square root of the watershed area, in order not to have deviations in runoff flows (i.e. 1 km resolution for a 10 km² watershed, 4 km resolution for a 100 km² watershed, as Segond et al. (2007) suggested). They considered catchments that varied in size from 30 to 100 km², which have been modelled using fully distributed rainfall–runoff models. Similarly, in this paper length scales are proposed for urban catchments, and adjusted and extended for application to semi-distributed drainage models (Table 2, Fig. 2). A scale dependency between storm, catchment and model topology for small scale urban catchments, is found based on the radar rainfall field using IDRA, with radar pixels mapped into square grids of 100 by 100 m, and into coarser resolutions, namely 500, 1000 and 2000 m, obtained by upscaling the original resolution. Results are analysed to investigate the effect of the amount of rainfall at different spatial resolutions on rainfall volume, peak runoff, and in-sewer water depths at locations inside the catchment, according to the dimensionless parameters specified.

3.1 Scale lengths

3.1.1 Storm and catchment lengths

To characterise storm size, de-correlation length of the storm C_D is defined as the distance from which rainfall rates are statistically independent. For each one of the four

HESSD

11, 5991–6033, 2014

Sensitivity of urban hydrodynamic modelling

G. Bruni et al.

Title Page

Abstract

Introduction

Conclusions

References

Tables

Figures

⏪

⏩

◀

▶

Back

Close

Full Screen / Esc

Printer-friendly Version

Interactive Discussion



Sewer length SW_L characterises the inter-pipe distance, thus the density of the sewer network; it is roughly the urban equivalent of drainage density for natural catchments. SW_L was defined as the ratio between catchment size and the total length of the piped system. Similar to RR_L , the condition $R_R \ll SW_L$ guarantees that the sewer pipe system routes the correct rainfall volume, previously transformed in runoff over the corresponding runoff area.

3.1.3 Definition of sub-catchments

The analysis involving model length scales was conducted at sub-catchment scale: the district was divided into 11 subcatchments (Fig. 2). In lowland areas, drainage systems are often interlinked and looped and flow direction changes over the course of a storm event as the system first fills and then starts routing the storm water. This implies that flow directions and sub-catchment boundaries are changeable and cannot be defined based on topography or network configuration. For this reasons sub-catchments were delineated according to flow magnitude in pipes: sub-catchment boundaries were defined based on small or zero flow in pipes under constant flow conditions during a long-lasting, uniform storm.

3.2 Dimensionless parameters

Using the length scales, dimensionless parameters were computed to analyse relationships between spatial characteristics of rainfall, those of the catchment and its hydrological response (Table 3). “Rainfall sampling number” was defined as the ratio between rainfall spatial resolution (R_R) and storm de-correlation length (C_D) in order to study rainfall gradient smoothing in terms of the relationship between the estimated rainfall field and the storm inherent structure. This parameter is similar to the “storm smearing” effect defined by Odgen and Julien (1994); it accounts for the deformation of the storm structure caused by rainfall measurements of coarser resolution than the storm length. As R_R tends to C_D , rain rates in high intensity regions tends to decrease, and

Sensitivity of urban hydrodynamic modelling

G. Bruni et al.

[Title Page](#)

[Abstract](#)

[Introduction](#)

[Conclusions](#)

[References](#)

[Tables](#)

[Figures](#)



[Back](#)

[Close](#)

[Full Screen / Esc](#)

[Printer-friendly Version](#)

[Interactive Discussion](#)



conversely adjacent regions, characterised by light rain, are subsequently affected by a rainfall rate increasing. The overall effect is a reduction of rainfall gradients. The second dimensionless parameter, “catchment sampling number”, was defined as the ratio between R_R and catchment length C_L . It accounts for rainfall transfer across catchment boundaries, as the rainfall spatial resolution approaches the size of the catchment. When the parameter exceeds 1, rainfall variability is not captured by the catchment. The third parameter is called “runoff sampling number”, which is the ratio between rainfall resolution and runoff resolution, and, similar to catchment sampling number, quantifies the correct assignment of rainfall values to the corresponding runoff area. The higher this ratio, the less precise is the rainfall assignment to the correct runoff area, but also the lower is the ratio, the more unable is the model to capture the rainfall variability, as the model resolution is coarser than the rainfall resolution. The fourth and last parameter is the “sewer sampling number”, composed by the ratio between the rainfall spatial resolution and the intra-sewer length. The lower the value of this parameter, the less sensitive is the drainage network to rainfall variability: a low “sewer sampling number” means that the inter-pipe distance, which represents the inverse of the density of the sewer network, is lower than the rainfall pixel size, so the sewer system cannot catch the rainfall variability described by the radar pixels. Conversely, as the ratio gets higher, the limiting factor becomes the rainfall resolution: the sewer model is sufficiently fine to capture the rainfall variability and route it through the piped system, but the rainfall input is too coarse, and this may result in lack of accuracy of the modelled water levels and sewer overflows.

To compare results between rainfall resolutions and between storms, model results were normalised with respect to the results of the case with the highest rainfall spatial resolution: total rainfall volumes, runoff peaks and maximum in-sewer water depths

HESSD

11, 5991–6033, 2014

Sensitivity of urban hydrodynamic modelling

G. Bruni et al.

[Title Page](#)

[Abstract](#)

[Introduction](#)

[Conclusions](#)

[References](#)

[Tables](#)

[Figures](#)



[Back](#)

[Close](#)

[Full Screen / Esc](#)

[Printer-friendly Version](#)

[Interactive Discussion](#)



were expressed as in Eqs. (2)–(4) respectively:

$$V_{\text{norm}}(R_{\text{Ri}}) = \frac{V(R_{\text{Ri}})}{V(100)} \quad (2)$$

$$Q_{\text{norm}}(R_{\text{Ri}}) = \frac{Q(R_{\text{Ri}})}{Q(100)} \quad (3)$$

$$\text{WD}_{\text{norm}}(R_{\text{Ri}}) = \frac{\text{WD}(R_{\text{Ri}})}{\text{WD}(100)} \quad (4)$$

4 Results and discussion

Computed model results of four storms were compared against dimensionless parameters to identify trends and variability as a function of storm characteristic, radar resolution, and model resolution.

4.1 Effect of spatial resolution

4.1.1 Catchment sampling number vs. rainfall total volume

The catchment sampling number describes the effect on rainfall volumes of rainfall transfer across basin boundaries due to rainfall spatial resolution coarsening. Figure 3 shows mean and standard deviation of the normalised rainfall volumes (Eq. 2) measured over the catchment, for all storms, vs. the catchment sampling number.

There is little change in the storm total rainfall volumes for $R_{\text{R}}/C_{\text{L}} < 0.2$; the normalised rainfall volume is close to 1, i.e. rainfall volumes are the same as in the reference case. For catchment sampling numbers larger than 0.2, both rainfall volume mean and standard deviation drop. This means that rainfall variability in volumes decrease and become more uniform within the district. This is caused by the smoothing effect induced by the resolution coarsening and its effect of displacement of the storm beyond the catchment boundaries (this effect is visualised in Fig. 1b). As a result

Title Page

Abstract

Introduction

Conclusions

References

Tables

Figures

⏪

⏩

◀

▶

Back

Close

Full Screen / Esc

Printer-friendly Version

Interactive Discussion



of the spatial averaging over an increasingly large area, the convective cells shift to a location that might no longer affect the catchment drainage area. According to the findings of Ogden and Julien (1994), this effect occurs by catchment sampling numbers greater than 0.4. In contrast, results of present study show that this effect already occurs at smaller sampling numbers, namely 0.2 and becomes noticeable for values greater than 0.2. Similar smoothing effect also becomes visible from the box plots of Fig. 4, where maximum rainfall intensity is plotted as a function of rainfall spatial resolution. The median of maximum intensity shows a mild decrease for coarser rainfall resolutions. The smoothing effect is more visible in Event 3 and Event 4, because of the distribution of convective cells at the edge of the catchment boundaries. The more delocalised the storm is with respect to the catchment centroid, the higher the effect of the rainfall shifting beyond the boundaries will be. Analysing each single event, in Event 1, the upper and lower quartiles are in the same range for spatial resolutions of 0.1 to 1 km. This shows that the decrease of the median is due to missed detection of extremely high rainfall intensities. The most extreme rainfall intensities are only captured at 100 m resolution (upper whisker in 100 m box plot, Fig. 4). Because Event 1 is characterised by 1 km-wide storm line passing over the catchment very rapidly, the spatial structure of the storm line is decomposed when resolution is coarsened beyond 1 km (see also Fig. 1b). For Event 2, the distance between the upper and lower quartiles in the box plots becomes smaller at the 1000 m scale, while the median does not change considerably. This means that at 1000 m resolution the convective storm cell structure is strongly smoothed and rainfall gradient decreases to an almost uniform distribution. Event 3 and Event 4 present a clear decreasing of the median along rainfall coarsening, with surprisingly higher variability, as indicated by 25–75 % range, at 1000 m resolution. In the first case, this is due to the non-organised structure of rainfall: localised rainfall peaks found in 100 m resolution are smoothed out at 500 m resolution, while at 1000 m resolution the convective area is found at the eastern boundary of the catchment, affecting 25 % of the area (2 pixels out of 9). In Event 4, the higher variability is due to the drop of lower quartile (10 mm h^{-1}), much lower than 100 and 500 m resolutions.

Sensitivity of urban hydrodynamic modelling

G. Bruni et al.

[Title Page](#)[Abstract](#)[Introduction](#)[Conclusions](#)[References](#)[Tables](#)[Figures](#)[Back](#)[Close](#)[Full Screen / Esc](#)[Printer-friendly Version](#)[Interactive Discussion](#)

in all events the median of the normalised runoff peaks is close to 1, showing a weak decrease with the coarsening of the rainfall resolution. Furthermore, there is more variability in normalised runoff peak compared to variability in in-sewer water depths, which implies that deviations in runoff results are smoothed by the sewer routing and storage and it results in lower deviation in in-sewer depths.

4.1.3 Spatial structure of rainfall: anisotropic semi-variogram

Figure 6 shows the experimental multi-directional spatial semi-variogram for each of the four events. For each storm and each time step, the semi-variogram has been calculated in 4 directions, from 0 to 180°, starting from north and going clockwise (direction at 0 and 180° are the same, thus plots coincide) at an angle step of 45°. To obtain a unique semi-variogram that was representative of the overall duration of the storm, for each direction, a weighted average of all semi-variograms has been computed, assigning a higher weight to those of higher variance. This criterion was chosen to focus the study on the highest rainfall intensity structure, without losing information on the temporal evolution of the storm. Rainfall data used for the calculation are those estimated at the highest temporal and spatial resolution of IDRA radar, 1 and 100 m respectively, in order to analyse rainfall structure at its most accurate description. The semi-variogram of Event 1 (Fig. 6 top left) presents a unique structure with a range of 1200 m in three out of four directions, while at 90° direction the range is smaller, reaching a de-correlation distance at 950 m. This is quite expected since Event 1 is a squall line moving from west to east, thus the gradient at 90° is steeper than at 180°. All four semi-variograms show a fast rise, although the shape of the one at 90° diverts considerably from the rest.

The same results if found for Event 2: the directional semi-variogram at 90° shows a faster rise than the rest of directions, thus the storm structure is highly oriented and defined. The de-correlation distance is 1000 m. Semi-variograms of Event 3 and 4 show a milder rise with respect to Event 1 and 2; they are characterised by a different rainfall structure type: Event 3 is a non-organised storm band, it seems to have a more defined

Sensitivity of urban hydrodynamic modelling

G. Bruni et al.

[Title Page](#)

[Abstract](#)

[Introduction](#)

[Conclusions](#)

[References](#)

[Tables](#)

[Figures](#)



[Back](#)

[Close](#)

[Full Screen / Esc](#)

[Printer-friendly Version](#)

[Interactive Discussion](#)



structure in 45° and 90° direction, the range of which is 1480 m (see also Table 3). The curve at 135° and 180° directions do not reach stability, meaning that the de-correlation distance exceeds the catchment size, within which the semi-variogram is calculated. Rainfall structure of Event 4 is more uniform, the four direction curves rise at almost the same rate, showing an almost isotropic behaviour. This is an expected result, since light rain storms are characterised by low and uniform rainfall rate. The de-correlation distance is 1600 m, the highest among the four events, found in 180° direction. No explanation was found to interpret the pronounced decrease in the semi-variogram of Event 1 and Event 2. We can only report that the same behaviour was found in storms belonging to the same rainfall group defined by Emmanuel et al. (2012). The de-correlation distances found by means of this geostatistical approach were used to compute the rainfall sampling number discussed in Sect. 4.1.4.

4.1.4 Rainfall sampling number vs. normalised in-sewer maximum water depth results

The rainfall sampling number is a measure for what Ogden and Julien (1994) call “storm smearing”: rainfall rates in convective regions tend to decrease while rain rates in low intensity regions tend to increase as a result to spatial aggregation. The overall effect is thus a flattening of rainfall gradients. This happens when the resolution of the volume unit measured by the weather radar approaches or exceeds the rainfall de-correlation length, thus the rainfall sampling number exceeds 1. Figure 7 shows the normalised maximum water depths against rainfall sampling number, at the outlet nodes of the 10 subcatchments and the outlet node of the whole catchment (catchment number 11 in Fig. 7). For all events, deviation in normalised water depth strongly increases for R_R/C_D between 0.5 and 1. For Event 1, when the ratio R_R/C_D exceeds 1, the deviation slightly reduces in 5 of out 11 catchments while it slightly increases for 6 subcatchments, depending on the local re-distribution of rainfall. Similar deviations were found for Event 2, this suggests that a R_R/C_D ratio between 0.5 and 1 is critical for “storm smearing”. Results are in agreement with the findings of Ogden and Julien (1994). They found for

Sensitivity of urban hydrodynamic modelling

G. Bruni et al.

Title Page

Abstract

Introduction

Conclusions

References

Tables

Figures



Back

Close

Full Screen / Esc

Printer-friendly Version

Interactive Discussion



their catchments that “storm smearing” occurred for $R_R/C_D > 0.8$. For both events, it can be noticed that one of the subcatchments shows a substantially different behaviour: for Event 1, sub-catchment 2 shows the highest deviation at $R_R/C_D = 0.5$, followed by a decrease for coarser resolutions. This is because the sub-catchment is located at the boundary of the storm. There, at 500 m spatial resolution rainfall gradient increases, while at 1000 m resolution the gradient shows a decrease due to the averaging with the upper region not affected by the storm. This directly affects the maximum water depth in sub-catchments. The opposite situation occurs in sub-catchment 5. A substantial increase of rainfall intensity is observed only at 2000 m resolution, where R_R/C_D equals 1.8. The sub-catchment is located in the southern part of the catchment with the closest node at 1.2 km from the convective region which is larger than the de-correlation length. The storm only affects the southern region when rainfall data is aggregated to the 2000 m resolution. The storm “virtually” shifts from the northern part of the catchment to the whole catchment area by the 2000 m averaging. A similar effect is noticed at the same sub-catchment for Event 2. In Event 3 and 4 rainfall smearing occurs at $R_R/C_D = 0.7$, deviations start to be relevant: normalised maximum water depths are between 0.98 and 1.06 in Event 3 and between 0.8 and 0.9 in Event 4. Summarizing all the results it has been found that beyond $R_R/C_D = 0.9$, and thus for rainfall resolution almost approaching the storm de-correlation length, rainfall gradient smoothing produces deviation effects on hydraulic outputs. In the case of the non-organized rainfall and light rain, the effect occurs later when rainfall resolution is at 70 % of the storm length. Therefore in this case, for localised rainfall events having length smaller than 900 m, the current resolution of operational weather radars (1000 m) is insufficient to have a proper estimation of intra-urban hydrological dynamics.

4.1.5 Runoff sampling number vs. normalised runoff peak results

Normalised maximum peaks of all runoff areas have been averaged within each one of the 11 catchments and plotted vs. the corresponding runoff sampling number (Fig. 8). Deviations from 100 m simulation remains between 0.9 and 1.1 for $R_R/RR_L < 20$, while

Sensitivity of urban hydrodynamic modelling

G. Bruni et al.

Title Page

Abstract

Introduction

Conclusions

References

Tables

Figures



Back

Close

Full Screen / Esc

Printer-friendly Version

Interactive Discussion



higher deviations up to almost 50% occur from $R_R/RR_L = 20$ on. In this case, the value $R_R/RR_L = 20$ means that deviations above 10% occur when the rainfall pixel size used to feed an urban hydrological model is 20 times larger than the runoff model resolution. For example, for simulations using the operational weather radar product of the Netherlands (1000 m), this would correspond to runoff area length of 50 m, satisfied in nine out of eleven catchments.

4.1.6 Sewer sampling number vs. normalised maximum water depth results

As presented in Sect. 3, sewer sampling number represents a measure of the ability of the sewer system to capture rainfall variability. For this case study, the intra-sewer pipe distance of the 11 catchments analysed is quite small, ranging from 33 m to 78 m: this means that there are 700 to 900 m of sewer pipes per 100 m² of catchment area, thus quite dense. The idea here is to give an indication not on the effect of spatial rainfall resolution alone on sewer model outputs, but of the combination of rainfall resolution and sewer model resolution. Results of deviations from the reference case averaged over all events are plotted in Fig. 9 against R_R/SW_L ; there is a decreasing trend of maximum water depths as the sewer sampling number increases: deviations are low when $R_R/SW_L < 10$, and increase when R_R/SW_L exceeds this value. Using again as example, when adopting the rainfall resolution provided by the national radar product, in order to have $R_R/SW_L = 10$ the intra-sewer length should not be greater than 100 m, requirement met for the catchments under study. In general, deviations from the reference case are smaller for in-sewer water depths, ranging from 0.87 to 1.13, than for runoff peaks, which are in the range 0.7–1.5. This is due to the smoothing effect of the flow routing through the pipe system.

Sensitivity of urban hydrodynamic modelling

G. Bruni et al.

[Title Page](#)

[Abstract](#)

[Introduction](#)

[Conclusions](#)

[References](#)

[Tables](#)

[Figures](#)

[⏪](#)

[⏩](#)

[⏴](#)

[⏵](#)

[Back](#)

[Close](#)

[Full Screen / Esc](#)

[Printer-friendly Version](#)

[Interactive Discussion](#)



4.2 Effects of temporal resolution

4.2.1 Changes in spatial structure of rainfall due to time aggregation

The X-band radar images are obtained at 1 min temporal scale: the radar completes radar scans in 1 min and an image covering 15 km range is delivered. In order to analyse the effect of temporal resolution on spatial anisotropic semi-variogram, raw rainfall data were aggregated to increasing time steps; rainfall rate images at different time resolutions were obtained by averaging the original images at 5 and 10 min. The anisotropic experimental semi-variogram was then computed based on the aggregated radar images (Fig. 10). Results show that the semi-variogram changes in shape when aggregating to 5 min, and shows very little change when moving from 5 to 10 min. Another consequence of the time aggregation is that the range increases: this is especially clear for Event 3 and Event 4; in the first case, at 5 and 10 min the storm structure within the catchment boundaries is lost, the semi-variogram are monotonic in any of the four directions considered. In Event 4, the range expands until the catchment limits for three out of four directions, while in 90° direction the semi-variogram has the same shape, and the range decreases. Event 1 and 2 seem less affected by the change in temporal resolution, the shape of the curves changes but the range expands only few tens of meters. Ranges function of time resolution are quantified in Table 4.

4.2.2 Effect in model results

Effect of the variation in rainfall temporal resolution on model outputs has been quantified through the comparison of time to maximum water depths. Figure 11 shows the time shift of maximum water depths between the reference simulation (100 m, 1 min) and both 5 min and 10 min simulations (both at 100 m spatial resolution). Results are shown at the outlets of the 11 subcatchments. Results show little sensitivity of the model to rainfall temporal resolution at 5 min and 10 min scales. As expected, time shift for 10 min simulation is larger than for 5 min simulation, although, for these 11 nodes,

HESSD

11, 5991–6033, 2014

Sensitivity of urban hydrodynamic modelling

G. Bruni et al.

Title Page

Abstract

Introduction

Conclusions

References

Tables

Figures



Back

Close

Full Screen / Esc

Printer-friendly Version

Interactive Discussion



5 it does not exceed 10 min (Fig. 11). The time shift has been calculated also for all the 3000 nodes of the catchment. When comparing the reference case with the 5 min simulation, only 0.64 % of nodes show a delay in maximum water depth between 5 min and 10 min, while for the rest of the nodes differences are smaller than 5 min. Looking at the comparison between reference case and 10 min simulation, 0.86 % of differences are between 5 min and 10 min, being the rest less than 5 min.

10 Event 3 and Event 4 have been simulated at two spatial and two temporal resolutions, namely 100 and 1000 m, and 5 and 10 min respectively. Figure 12 shows results in maximum water depth time shift with respect to reference cases (100 m and 1 min, and 1000 m and 1 min). In Event 3 simulation, results show that the model is most sensitive at 100 m/10 min resolution pairs. Time delay of maximum water depths from reference case is between 8 and 16 min. When coarsening the spatial resolution, the impact on results is lower, and increases by increasing the rainfall time aggregation. The relatively high impact of 100 m and 10 min resolution simulation is explained by the change of the rainfall structure; see also Fig. 10 third line. Correlation length becomes larger than the catchment size starting from 5 min aggregation, but it has an effect in model results only at 10 min aggregation. In both cases the time aggregation results in an enlargement of the area affected by convective storm cells, in a smoothing of rainfall peaks, and mostly in a delay/anticipation of rainfall peaks, which results in a delay/anticipation of maximum water depths, depending on the relative position of the node to the storm. One reason that explains why this effect is noticeable only at 10 min is because the concentration time of the 11 nodes is lower than 10 min. In order to notice an impact on model output, the time-step must be smaller than the concentration time of the catchment at the outlet (Vaes et al., 2001) (being the concentration time the time rainfall needs to travel from the furthest place in the catchment to the chosen outlet of the sewer system). Moreover, the sensitivity of the model is low to temporal aggregation performed on 1000 m spatial aggregation data. In Event 4, an anticipation of maximum water depths occurs as effect of the rainfall temporal aggregation, but again the sensitivity of the model is low: time shift is under 5 min, except for

Sensitivity of urban hydrodynamic modelling

G. Bruni et al.

[Title Page](#)[Abstract](#)[Introduction](#)[Conclusions](#)[References](#)[Tables](#)[Figures](#)[Back](#)[Close](#)[Full Screen / Esc](#)[Printer-friendly Version](#)[Interactive Discussion](#)

catchment 6 and 10, for which is 6 min. Moreover, effects of time aggregation on model performance have been analysed through the comparison in maximum water depths between simulations. However, due to the low deviations found, results have not been reported here.

5 Conclusions

The sensitivity of a semi-distributed hydrodynamic model to spatial and temporal resolutions of weather radar data was investigated in this paper. Analysed are based on a densely populated urban catchment in Rotterdam, the Netherlands. Rainfall and catchment were characterised using various length scales: catchment size and storm de-correlation length, which depend on the specific site and storm; rainfall data resolution, which depends on rainfall measurement resolution; and runoff resolution and sewer density, which are modeller's choices. Sensitivity of the model to rainfall spatial resolution was analysed in relation with: catchment size, through catchment sampling number (R_R/C_L); storm length, by means of rainfall sampling number (R_R/C_D); runoff resolution of the model, through runoff sampling number (R_R/RR_L); and sewer density, with the sewer sampling number (R_R/SW_L). The first parameter is responsible for the uncertainty of rainfall location with respect to the watershed boundaries; the second parameter describes the decrease in rain rate gradients; the third and the fourth parameters describe the ability of the model (the runoff model and the sewer model respectively) to capture the rainfall structure. The storm length has been computed as the range of the anisotropic experimental semi-variogram. Four rainfall spatial resolutions (100, 500, 1000 and 2000 m) and three temporal resolutions (1, 5 and 10 min) have been analysed. Results obtained by this analysis show:

- For $R_R/C_L > 0.2$, there is a progressive decrease of both rainfall volume mean and standard deviation: rainfall gradients decrease. This is the result of the smoothing effect of rainfall resolution coarsening and of the storm core displacement beyond

HESD

11, 5991–6033, 2014

Sensitivity of urban hydrodynamic modelling

G. Bruni et al.

Title Page

Abstract

Introduction

Conclusions

References

Tables

Figures

⏪

⏩

◀

▶

Back

Close

Full Screen / Esc

Printer-friendly Version

Interactive Discussion



the catchment boundaries. Spatial resolution effect strongly depends on the location of storm cells relative to the catchment.

- For $R_R/C_D > 0.9$, “rainfall smearing” occurs, inducing deviations in maximum modelled in-sewer water depths. For rainfall resolutions exceeding the storm de-correlation length, the flattening of rainfall gradients do have an impact on model performance, and its magnitude depends both on the type of rainfall and on how much the rainfall field is de-structured by the coarsening.
- For $R_R/RR_L > 20$, deviations in runoff peaks occur above 10%. This means that, in this case, when operational weather radar product are used to feed the model (1000 m spatial resolution), runoff area resolution lower than 50 m would cause an impact on runoff model outputs.
- For $R_R/SW_L > 10$, maximum water level depths start diverting from the reference case (100 m resolution). However, deviations are small, i.e. of the order of 10% at most. In general there is a low impact on sewer model outputs due to rainfall spatial coarsening, due mainly to the smoothing effect of the flow routing through the pipe system.

Moreover, an analysis of the change in spatial structure of rainfall due to time aggregation has been conducted, and therefore of the impact on model results has been quantified in terms of time shift of maximum water depths with respect to the reference case, i.e. 1 min temporal resolution simulation. The experimental anisotropic semi-variograms computed for the three temporal aggregations show how rainfall field structure changes due to the temporal resolution coarsening. In general it affects the rainfall correlation length, which increases along with time aggregation. Model performance is affected by rainfall aggregation only when the rain field is completely distorted, this happens only in case of Event 3. More generally, the model smoothes the rainfall field variation caused by the temporal aggregation, and it results in peaks time shift generally lower than 6 min.

Sensitivity of urban hydrodynamic modelling

G. Bruni et al.

[Title Page](#)

[Abstract](#)

[Introduction](#)

[Conclusions](#)

[References](#)

[Tables](#)

[Figures](#)



[Back](#)

[Close](#)

[Full Screen / Esc](#)

[Printer-friendly Version](#)

[Interactive Discussion](#)



This is a first attempt to characterise how the various rainfall structures affect the hydrological modelling of urban catchments, and how the rainfall change in resolution is absorbed by the model, giving indication on the scale relationship between the resolution of the main component affecting the modelling: storm structure, its representation, catchment size, and model resolution. To give a more robust meaning to these sampling numbers, more storm events should be analysed to confirm the findings of this study. Such an extension of the study would allow giving reliable recommendations on what should be the model and rainfall resolution in order to prioritise either the improvement on rainfall estimation or catchment hydrological characterization.

Acknowledgements. This work has been funded by the EU INTERREG IVB RainGain Project. The authors would like to thank the RainGain Project for supporting this research (www.raingain.eu).

References

- Balmforth, D. J. and Dibben, P.: A Modelling Tool for Assessing Flood Risk, Water Practice & Technology, IWA, doi:10.2166/WPT.2006.008, 2006.
- Bell, V. A. and Moore, R. J.: The sensitivity of catchment runoff models to rainfall data at different spatial scales, Hydrol. Earth Syst. Sci., 4, 653–667, doi:10.5194/hess-4-653-2000, 2000.
- Berne, A., Delrieu, G., Creutin, J.-D., and Obled, C.: Temporal and spatial resolution of rainfall measurements required for urban hydrology, J. Hydrol., 299, 166–179, doi:10.1016/j.jhydrol.2004.08.002, 2004.
- Blanchet, F., Brunelle, D., and Guillon, A.: Influence of the spatial heterogeneity of precipitation upon the hydrologic response of an urban catchment, 2nd Int. Symp. Hydrological Applications of Weather Radar, Hannover, 450–457, 1992.
- Dawdy, D. R. and Bergmann, J. M.: Effect of rainfall variability on streamflow simulation, Water Resour. Res., 5, 958–966, 1969.
- Deltares: Sobek Suite V2.13, Deltares, Delft, NL, available at: http://content.oss.deltares.nl/delft3d/manuals/SOBEK_User_Manual.pdf, 2014.

HESSD

11, 5991–6033, 2014

Sensitivity of urban hydrodynamic modelling

G. Bruni et al.

Title Page

Abstract

Introduction

Conclusions

References

Tables

Figures



Back

Close

Full Screen / Esc

Printer-friendly Version

Interactive Discussion



Sensitivity of urban hydrodynamic modelling

G. Bruni et al.

[Title Page](#)

[Abstract](#)

[Introduction](#)

[Conclusions](#)

[References](#)

[Tables](#)

[Figures](#)

[⏪](#)

[⏩](#)

[◀](#)

[▶](#)

[Back](#)

[Close](#)

[Full Screen / Esc](#)

[Printer-friendly Version](#)

[Interactive Discussion](#)



- Einfalt, T., Arnbjerg-Nielsen, K., Golz, C., Jensen, N.-E., Quirmbach, M., Vaes, G., and Vieux, B.: Towards a roadmap for use of radar rainfall data in urban drainage, *J. Hydrol.*, 299, 186–202, doi:10.1016/j.jhydrol.2004.08.004, 2004.
- Emmanuel, I., Andrieu, H., Leblois, E., and Flahaut, B.: Temporal and spatial variability of rainfall at the urban hydrological scale, *J. Hydrol.*, 430–431, 162–172, doi:10.1016/j.jhydrol.2012.02.013, 2012.
- Gires, A., Onof, C., Maksimovic, C., Schertzer, D., Tchiguirinskaia, I., and Simoes, N.: Quantifying the impact of small scale unmeasured rainfall variability on urban runoff through multifractal downscaling: a case study, *J. Hydrol.*, 442–443, 117–128, doi:10.1016/j.jhydrol.2012.04.005, 2012.
- Gires, A., Tchiguirinskaia, I., Schertzer, D., and Lovejoy, S.: Multifractal analysis of a semi-distributed urban hydrological model, *Urban Water J.*, 10, 195–208, doi:10.1080/1573062X.2012.716447, 2013.
- Jensen, N. E. and Pedersen, L.: Spatial variability of rainfall: variations within a single radar pixel, *Atmos. Res.*, 77, 269–277, doi:10.1016/j.atmosres.2004.10.029, 2005.
- Koren, V., Finnerty, B., Schaake, J., Smith, M., Seo, D.-J., and Duan, Q.-Y.: Scale dependencies of hydrologic models to spatial variability of precipitation, *J. Hydrol.*, 217, 285–302, doi:10.1016/S0022-1694(98)00231-5, 1999.
- Krajewski, W. F., Lakshmi, V., Georgakakos, K. P., and Jain, S. C.: A Monte Carlo study of rainfall sampling effect on a distributed catchment model, *Water Resour. Res.*, 27, 119–128, 1991.
- Leijnse, H., Uijlenhoet, R., van de Beek, C. Z., Overeem, A., Otto, T., Unal, C. M. H., Dufournet, Y., Russchenberg, H. W. J., Figueras i Ventura, J., Klein Baltink, H., and Holleman, I.: Precipitation measurement at CESAR, the Netherlands, *J. Hydrometeorol.*, 11, 1322–1329, doi:10.1175/2010JHM1245.1, 2010.
- Liguori, S., Rico-Ramirez, M. A., Schellart, A. N. A., and Saul, A. J.: Using probabilistic radar rainfall nowcasts and NWP forecasts for flow prediction in urban catchments, *Atmos. Res.*, 103, 80–95, doi:10.1016/j.atmosres.2011.05.004, 2012.
- Matheron, G.: Principles of geostatistics, *Econ. Geol.*, 58, 1246–1266, 1963.
- Neal, J., Villanueva, I., Wright, N., Willis, T., Fewtrell, T., and Bates, P.: How much physical complexity is needed to model flood inundation?, *Hydrol. Process.*, 26, 2264–2282, doi:10.1002/hyp.8339, 2012.

Sensitivity of urban hydrodynamic modelling

G. Bruni et al.

[Title Page](#)

[Abstract](#)

[Introduction](#)

[Conclusions](#)

[References](#)

[Tables](#)

[Figures](#)



[Back](#)

[Close](#)

[Full Screen / Esc](#)

[Printer-friendly Version](#)

[Interactive Discussion](#)



- Ogden, F. L. and Julien, P. Y.: Runoff model sensitivity to radar rainfall resolution, *J. Hydrol.*, 158, 1–18, 1994.
- Otto, T. and Russchenberg, H. W. J.: Estimation of specific differential phase and differential backscatter phase from polarimetric weather radar measurements of rain, *IEEE Geosci. Remote S.*, 8, 988–992, doi:10.1109/LGRS.2011.2145354, 2011.
- Ozdemir, H., Sampson, C. C., de Almeida, G. A. M., and Bates, P. D.: Evaluating scale and roughness effects in urban flood modelling using terrestrial LIDAR data, *Hydrol. Earth Syst. Sci.*, 17, 4015–4030, doi:10.5194/hess-17-4015-2013, 2013.
- Parker, D. J., Priest, S. J., and McCarthy, S. S.: Surface water flood warnings requirements and potential in England and Wales, *Appl. Geogr.*, 31, 891–900, doi:10.1016/j.apgeog.2011.01.002, 2011.
- Pathirana, A., Tsegaye, S., Gersonius, B., and Vairavamorthy, K.: A simple 2-D inundation model for incorporating flood damage in urban drainage planning, *Hydrol. Earth Syst. Sci.*, 15, 2747–2761, doi:10.5194/hess-15-2747-2011, 2011.
- Priest, S. J., Parker, D. J., Hurford, A. P., Walker, J., and Evans, K.: Assessing options for the development of surface water flood warning in England and Wales., *J. Environ. Manage.*, 92, 3038–48, doi:10.1016/j.jenvman.2011.06.041, 2011.
- Schellart, A. N. A., Shepherd, W. J., and Saul, A. J.: Influence of rainfall estimation error and spatial variability on sewer flow prediction at a small urban scale, *Adv. Water Resour.*, 45, 65–75, doi:10.1016/j.advwatres.2011.10.012, 2012.
- Schmitt, T. G., Thomas, M., and Ettrich, N.: Analysis and modeling of flooding in urban drainage systems, *J. Hydrol.*, 299, 300–311, doi:10.1016/j.jhydrol.2004.08.012, 2004.
- Segond, M.-L., Wheeler, H. S., and Onof, C.: The significance of spatial rainfall representation for flood runoff estimation: a numerical evaluation based on the Lee catchment, UK, *J. Hydrol.*, 347, 116–131, doi:10.1016/j.jhydrol.2007.09.040, 2007.
- Seliga, T. A., Aron, G., Aydin, K., and White, E.: Storm runoff simulation using radar-estimated rainfall rates and a Unit Hydrograph model (SYN-HYD) applied to the GREVE watershed, in: *Am. Meteorol. Soc.*, 25th Int. Conf. on Radar Hydrology, 587–590, preprint, 1992.
- Stichting RIONED: Rioleringsberekeningen, hydraulisch functioneren, Leidraad Riolerings (Dutch Guidelines for sewer systems computations and hydraulic functioning) (in Dutch). Stichting RIONED – National centre of expertise in sewer management and urban drainage in the Netherlands, the Netherlands, doi:10.1016/j.advwatres.2011.10.012, 2004.

Sensitivity of urban hydrodynamic modelling

G. Bruni et al.

Title Page

Abstract

Introduction

Conclusions

References

Tables

Figures

⏪

⏩

◀

▶

Back

Close

Full Screen / Esc

Printer-friendly Version

Interactive Discussion



Storm, B. A., Parker, M. D., and Jorgensen, D. P.: A convective line with leading stratiform precipitation from BAME X., *Mon. Weather Rev.*, 135, 1769–1785 doi:10.1175/MWR3392.1, 2007.

5 Vaes, G., Willems, P., and Berlamont, J.: Rainfall input requirements for hydrological calculations, *Urban Water J.*, 3, 107–112, doi:10.1016/S1462-0758(01)00020-6, 2001.

Vieux, B. E. and Imgarten, J. M.: On the scale-dependent propagation of hydrologic uncertainty using high-resolution X-band radar rainfall estimates, *Atmos. Res.*, 103, 96–105, doi:10.1016/j.atmosres.2011.06.009, 2012.

10 Weisman, M. L. and Rotunno, R.: “A theory for strong long-lived squall lines” revisited, *J. Atmos. Sci.*, 61, 361–382, doi:10.1175/1520-0469(2004)061<0361:ATFSLS>2.0.CO;2, 2004.

Winchell, M., Gupta, H. V., and Sorooshian, S.: On the simulation of infiltration-and saturation-excess runoff using radar-based rainfall estimates: effects of algorithm uncertainty and pixel aggregation, *Water Resour. Res.*, 34, 2655–2670, 1998.

15 Wood, S. J., Jones, D. A., and Moore, R. J.: Static and dynamic calibration of radar data for hydrological use, *Hydrol. Earth Syst. Sci.*, 4, 545–554, doi:10.5194/hess-4-545-2000, 2000.

Sensitivity of urban hydrodynamic modelling

G. Bruni et al.

Table 4. Range per rainfall temporal aggregation, for all events. Ranges are calculated for the same directions of 1 min ranges.

Rainfall	Range (m)		
	$\Delta t = 1 \text{ min}$	$\Delta t = 5 \text{ min}$	$\Delta t = 10 \text{ min}$
Event 1	950	960	970
Event 2	1000	1200	1450
Event 3	1480	> 2000	> 2000
Event 4	1600	1500	1500

[Title Page](#)
[Abstract](#)
[Introduction](#)
[Conclusions](#)
[References](#)
[Tables](#)
[Figures](#)
[⏪](#)
[⏩](#)
[◀](#)
[▶](#)
[Back](#)
[Close](#)
[Full Screen / Esc](#)
[Printer-friendly Version](#)
[Interactive Discussion](#)


Sensitivity of urban hydrodynamic modelling

G. Bruni et al.

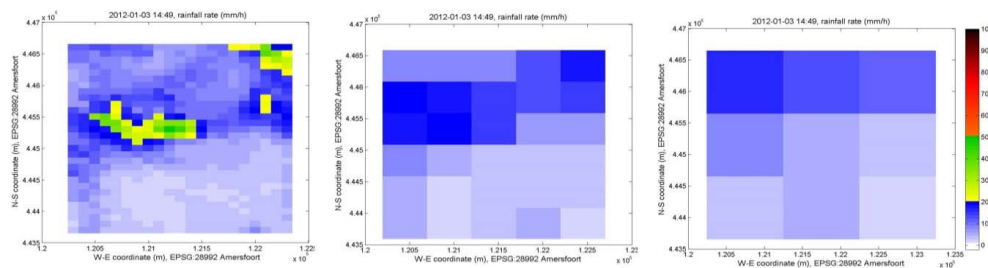


Figure 1b. Plots of the maximum intensity time step for Event 1 and for 3 rainfall resolutions (100 m, 500 m and 1000 m at left, centre and right side respectively). Moving to coarser resolution results in gradient smoothing and storm core displacement.

[Title Page](#)[Abstract](#)[Introduction](#)[Conclusions](#)[References](#)[Tables](#)[Figures](#)[Back](#)[Close](#)[Full Screen / Esc](#)[Printer-friendly Version](#)[Interactive Discussion](#)

Sensitivity of urban hydrodynamic modelling

G. Bruni et al.

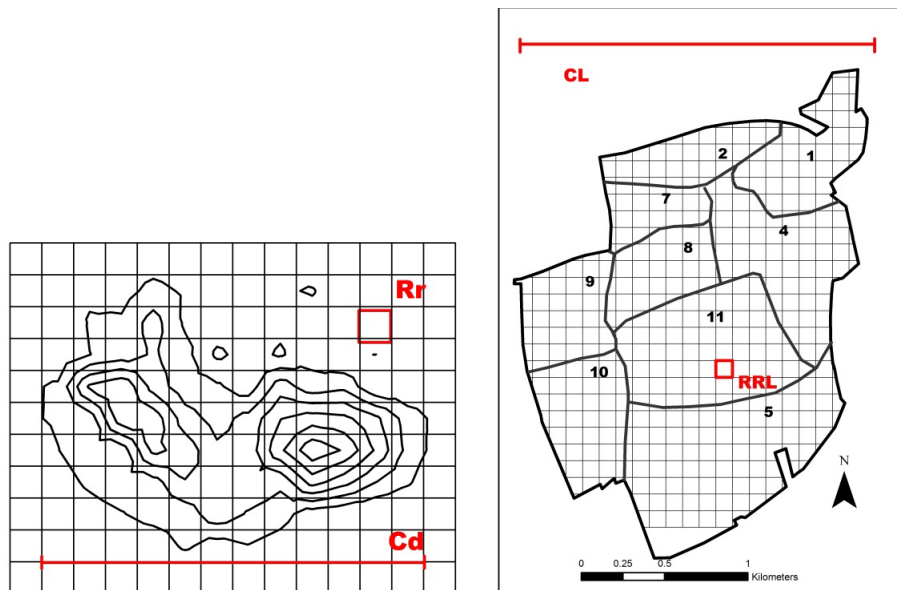


Figure 2. Storm de-correlation length (C_D) and rainfall resolution (R_R) in left panel; Catchment length (C_L), runoff length (RR_L) in right panel; the catchment is divided into 11 independent subcatchments.

[Title Page](#)[Abstract](#)[Introduction](#)[Conclusions](#)[References](#)[Tables](#)[Figures](#)[◀](#)[▶](#)[◀](#)[▶](#)[Back](#)[Close](#)[Full Screen / Esc](#)[Printer-friendly Version](#)[Interactive Discussion](#)

Sensitivity of urban hydrodynamic modelling

G. Bruni et al.

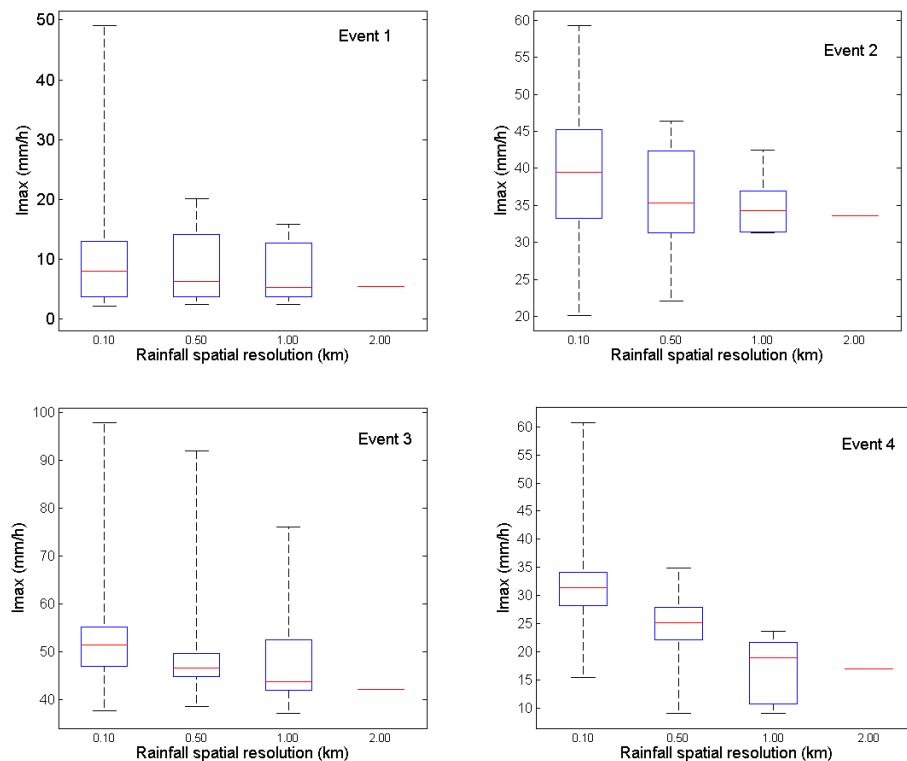


Figure 4. Box plots of maximum rainfall intensity (mm h^{-1}) among all pixels covering the catchment area, for the 4 spatial resolutions (the 2000 m shows a unique value being rainfall uniformly distributed all over the catchment), for the four events analysed.

Sensitivity of urban hydrodynamic modelling

G. Bruni et al.

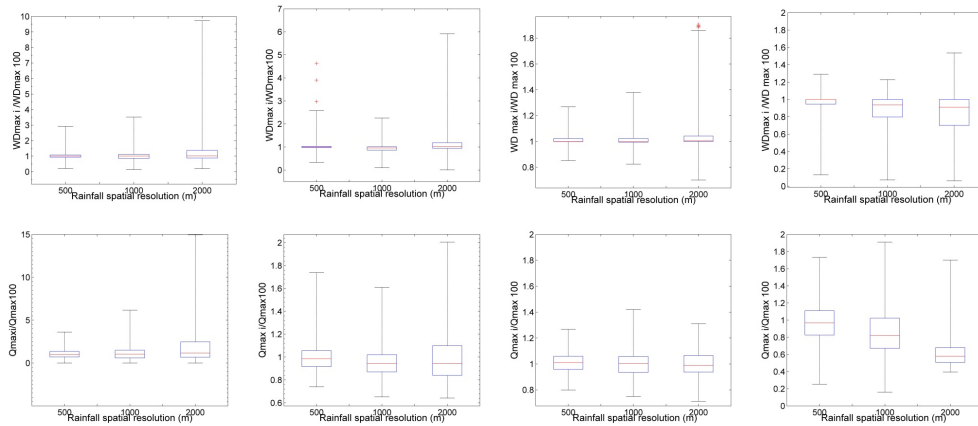


Figure 5. Box plot of the normalised water depths (top panel) and runoff peaks (bottom panel) for Events 1 to 4.

[Title Page](#)

[Abstract](#)

[Introduction](#)

[Conclusions](#)

[References](#)

[Tables](#)

[Figures](#)



[Back](#)

[Close](#)

[Full Screen / Esc](#)

[Printer-friendly Version](#)

[Interactive Discussion](#)



Sensitivity of urban hydrodynamic modelling

G. Bruni et al.

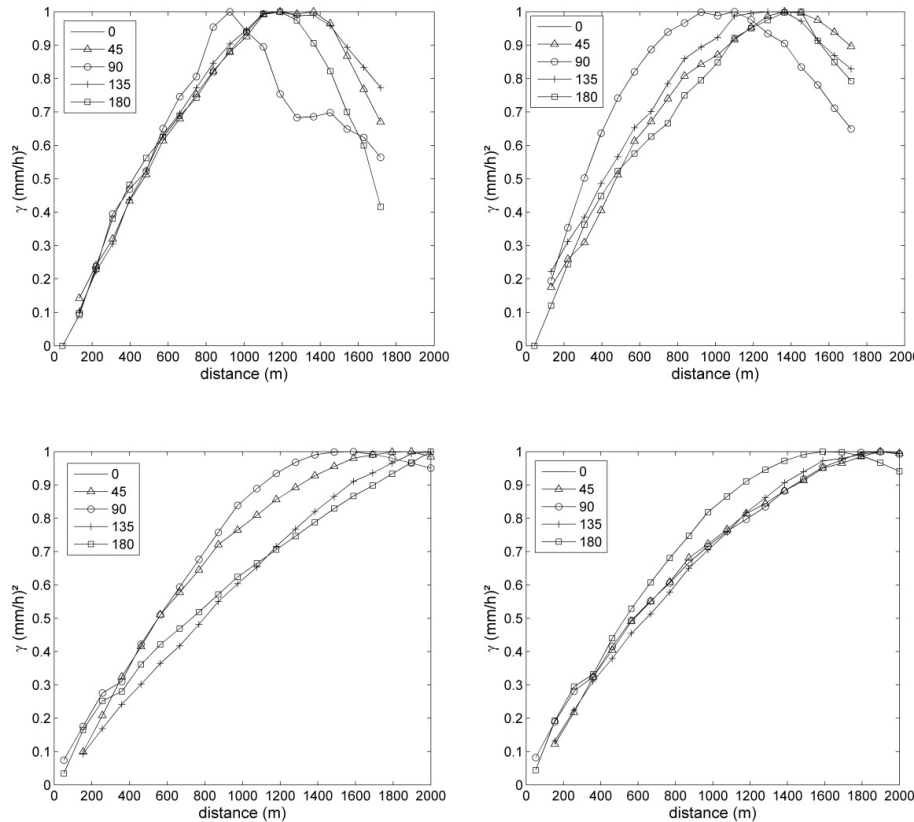


Figure 6. Instantaneous experimental multi-directional spatial semi-variogram of non-zero rainfall for each of the four storms (Events 1 and 2 top panel, Events 3 and 4 bottom panel).

[Title Page](#)
[Abstract](#) [Introduction](#)
[Conclusions](#) [References](#)
[Tables](#) [Figures](#)
 [◀](#) [▶](#)
 [◀](#) [▶](#)
[Back](#) [Close](#)
[Full Screen / Esc](#)
[Printer-friendly Version](#)
[Interactive Discussion](#)



Sensitivity of urban hydrodynamic modelling

G. Bruni et al.

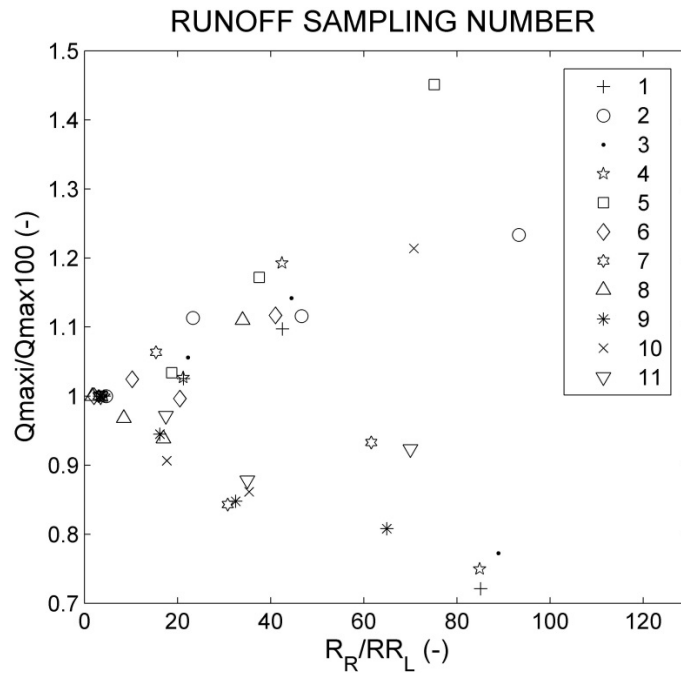


Figure 8. Runoff sampling number (R_R/RR_L) vs. normalised runoff peaks: results averaged over each of the 11 catchments.

Title Page

Abstract

Introduction

Conclusions

References

Tables

Figures



Back

Close

Full Screen / Esc

Printer-friendly Version

Interactive Discussion



Sensitivity of urban hydrodynamic modelling

G. Bruni et al.

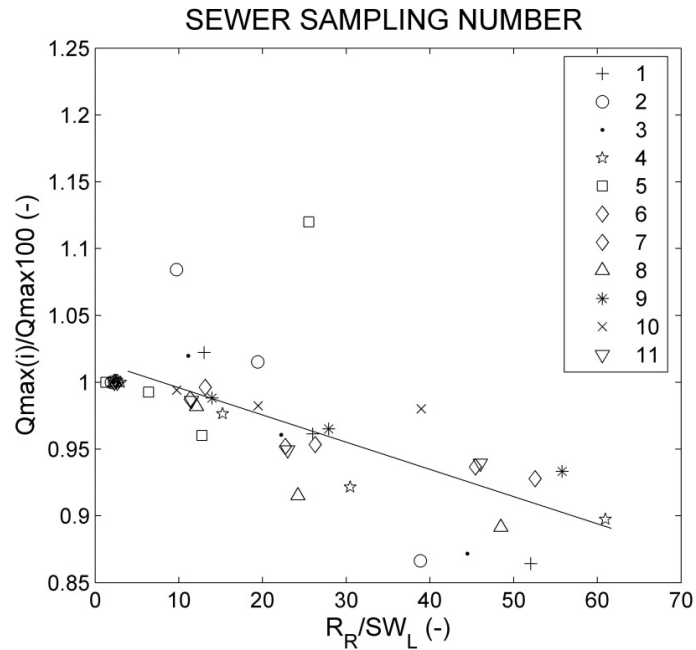


Figure 9. Sewer sampling number (R_R/SW_L) vs. normalised maximum water depths: results at the outlet of the 11 catchments.

[Title Page](#)[Abstract](#)[Introduction](#)[Conclusions](#)[References](#)[Tables](#)[Figures](#)[◀](#)[▶](#)[◀](#)[▶](#)[Back](#)[Close](#)[Full Screen / Esc](#)[Printer-friendly Version](#)[Interactive Discussion](#)

Sensitivity of urban hydrodynamic modelling

G. Bruni et al.

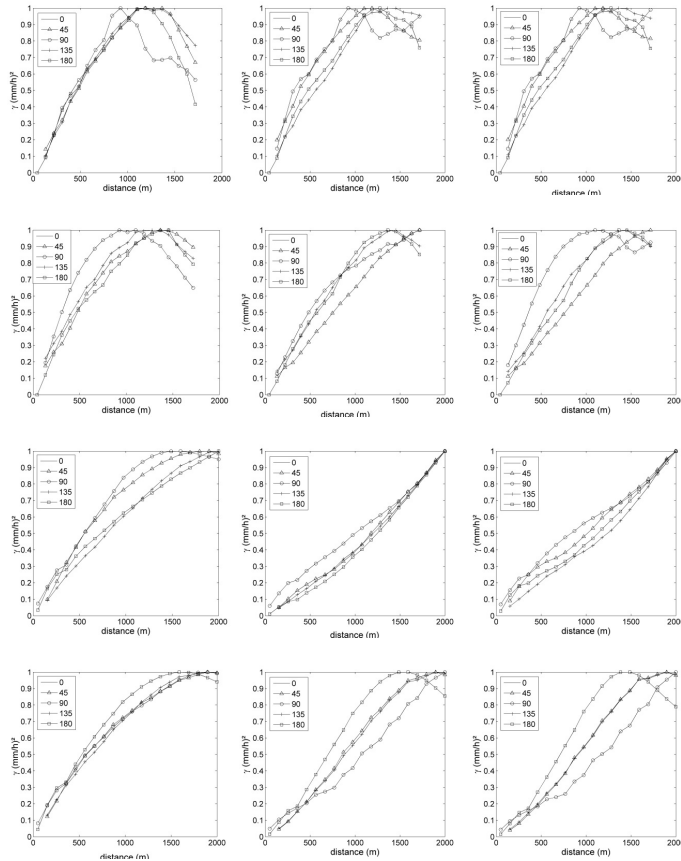


Figure 10. Anisotropic experimental semi-variogram for the four rainfall events (in rows) and different temporal resolutions, 1 min, 5 min and 10 min (left, central and right column respectively).

[Title Page](#)

[Abstract](#)

[Introduction](#)

[Conclusions](#)

[References](#)

[Tables](#)

[Figures](#)



[Back](#)

[Close](#)

[Full Screen / Esc](#)

[Printer-friendly Version](#)

[Interactive Discussion](#)



